J Physiol 589.4 (2011) pp 903–917

The Journal of Physiology

Regulation of visceral sympathetic tone by A5 noradrenergic neurons in rodents

Roy Kanbar, Seth D. Depuy, Gavin H. West, Ruth L. Stornetta and Patrice G. Guyenet

Department of Pharmacology, University of Virginia, Charlottesville, VA 22908, USA

Non-technical summary Patients suffering from obstructive sleep apnoea (OSA) experience repeated decreases in blood oxygen (hypoxia) and increases in CO_2 (hypercapnia) causing sleep disruption, cardiac over-stimulation, intense vasoconstriction and, eventually, day-time hypertension. Hypoxia and hypercapnia initiate these responses by activating the carotid bodies whereas hypercapnia also works in the central nervous system. In this study in anaesthetized rats we show that a group of noradrenergic neurons located in the lower brainstem (A5 neurons) are vigorously activated by carotid body stimulation and mildly affected by CO_2. We also show that selective activation of the A5 neurons increases sympathetic tone to the viscera and we suggest that these catecholaminergic neurons contribute to the cardiovascular stimulation caused by acute hypoxia. The importance of the A5 neurons to acute hypoxic responses in the conscious state remains to be assessed and their contribution to the day-time hypertension associated with OSA is also a matter for future research.

Abstract The ventrolateral pons contains the A5 group of noradrenergic neurons which regulate the circulation and probably breathing. The present experiments were designed to identify these neurons definitively *in vivo*, to examine their response to chemoreceptor stimuli (carotid body stimulation and changes in brain pH) and to determine their effects on sympathetic outflow. Bulbospinal A5 neurons, identified by juxtacellular labelling in anaesthetized rats, had a slow regular discharge, were vigorously activated by peripheral chemoreceptor stimulation with cyanide, but only mildly activated by hyperoxic hypercapnia (central chemoreceptor stimulation). The caudal end of the A5 region also contained neurons with properties reminiscent of retrotrapezoid neurons. These cells lacked a spinal axon and were characterized by a robust response to CO_2. The pH sensitivity of A5 neurons, examined in brain slices from neonatal (postnatal days 6–10) tyrosine hydroxylase (TH)-GFP transgenic mice, was about 10 times smaller than that of similarly recorded retrotrapezoid neurons. Selective stimulation of the A5 neurons in rats using channelrhodopsin optogenetics (A5 TH neurons represented 66% of transfected cells) produced fivefold greater activation of the renal nerve than the lumbar sympathetic chain. In summary, adult A5 noradrenergic neurons are vigorously activated by carotid body stimulation. This effect presumably contributes to the increase in visceral sympathetic nerve activity elicited by acute hypoxia. A5 neurons respond weakly to hypercapnia *in vivo* or to changes in pH in slices suggesting that their ability to sense local variations in brain pH or P_{CO_2} is limited.

(Received 23 August 2010; accepted after revision 13 December 2010; first published online 20 December 2010)
Corresponding author P. G. Guyenet: University of Virginia Health System, PO Box 800735, 1300 Jefferson Park Avenue, Charlottesville, VA 22908-0735, USA. Email: pgg@virginia.edu

Abbreviations BP, blood pressure; ChR2, channelrhodopsin-2; ir, immunoreactive; RTN, retrotrapezoid nucleus; SND, sympathetic nerve discharge; TH, tyrosine hydroxylase.

DOI: 10.1113/jphysiol.2010.198374

Introduction

Located in the ventrolateral pons, the A5 group of noradrenergic neurons have spinal projections that target almost exclusively the intermediolateral cell column (Loewy *et al.* 1979*b*; Byrum & Guyenet, 1987). Far less investigated than the noradrenergic neurons of the locus coeruleus (A6 group), the A5 neurons are suspected to regulate primarily the autonomic nervous system and respiration (Koshiya & Guyenet, 1994; Hilaire *et al.* 2004; Zanella *et al.* 2006; Li *et al.* 2008). Bulbospinal neurons located in the ventrolateral pons have been sporadically recorded *in vivo* in anaesthetized rats since 1982 (Andrade & Aghajanian, 1982; Byrum *et al.* 1984; Huangfu *et al.* 1991; Guyenet *et al.* 1993). These neurons have a slow regular resting discharge and spinal axons that arborize in or very close to the intermediolateral cell column. These cells are activated by nociceptive stimuli, inhibited by administration of α_2 adrenergic receptor agonists, inhibited or unaffected by increases in blood pressure, activated by hypoxia and display central respiratory modulation (Andrade & Aghajanian, 1982; Byrum *et al.* 1984; Huangfu *et al.* 1991; Guyenet *et al.* 1993). Although these properties are not highly discriminative, they provided reasonably convincing evidence that these cells could be the A5 noradrenergic neurons (Andrade & Aghajanian, 1982; Byrum *et al.* 1984; Huangfu *et al.* 1991; Guyenet *et al.* 1993). Our first objective was to ascertain that this interpretation is correct by testing whether ventrolateral pontine bulbospinal neurons with the above-described location and firing characteristics express tyrosine hydroxylase.

The locus coeruleus (A6 group) is a wake-promoting structure implicated in innumerable aspects of brain function including central respiratory chemoreception, the increase in breathing caused by a rise in brain P_{CO_2} or acidity (Aston-Jones *et al.* 1999, 2001; Nattie & Li, 2009). The locus coeruleus is suspected to contribute to respiratory chemoreception because of its ability to respond to brain parenchymal acidification and because bilateral lesion of this structure attenuates the breathing stimulation elicited by hypercapnia (Pineda & Aghajanian, 1997; Biancardi *et al.* 2008; Hartzler *et al.* 2008; Nattie & Li, 2009). The similarity between the known cellular properties of A5 and A6 neurons *in vivo* and *in vitro* raises the question of whether the A5 neurons also have the ability to respond to hypercapnia via an intrinsic sensitivity to acid. We address this question presently by testing whether the A5 neurons respond to hypercapnia *in vivo* and to acidification in slices.

Electrical stimulation, microinjection of glutamate receptor agonists or injection of muscimol have been used to delineate the role of the A5 noradrenergic neurons in anaesthetized and conscious mammals (Loewy *et al.* 1979*a*; Neil & Loewy, 1982; Stanek *et al.* 1984; Maiorov *et al.* 1999, 2000). These interventions produced a complex pattern of cardiovascular changes usually characterized by visceral vasoconstriction, increased skeletal muscle blood flow and small increases or decreases in blood pressure. The specific contribution of the A5 neurons to these effects has not been clearly established. The main stumbling block has always been that A5 neurons are few and scattered. In addition these cells reside in close proximity to the superior olivary complex, the deep layers of the trigeminal complex and the reticular formation which contain incomparably larger numbers of neurons that are unavoidably impacted by microinjecting neuronal depolarizing or hyperpolarizing agents amongst the A5 neurons. The third objective of the present study was to determine the cardiovascular effects produced by selective stimulation of the A5 neurons. To do so, we used an optogenetic approach based on the use of a lentiviral vector that expresses channelrhodopsin-2 (ChR2) under the control of the catecholaminergic neuron-preferring promoter PRSx8 (Hwang *et al.* 2001; Duale *et al.* 2007; Abbott *et al.* 2009*a*,*b*).

Methods

Animal use was in accordance with guidelines approved by the University of Virginia Animal Care and Use Committee (ACUC). All *in vivo* experiments were done on male Sprague–Dawley rats ($n = 19$) that were between 8 and 12 weeks old at the time of physiological recording. *In vitro* experiments were done on mouse brain slices. Six- to 10-day-old pups from TH-GFP transgenic mice (Matsushita *et al.* 2002) were used for this purpose.

In vivo electrophysiology

Anaesthesia was induced with 5% isoflurane in 100% oxygen. Artificial ventilation with 3% isoflurane in 100% oxygen was maintained throughout surgery. On completion of surgical preparation, isoflurane was reduced (1.8–2.0%) or gradually replaced by urethane (1.3 g kg^{-1}, I.V.) during physiological recording. Adequate anaesthesia was monitored by the absence of withdrawal reflex and blood pressure (BP) changes to a firm paw pinch. After administration of a neuromuscular blocking agent (pancuronium 1.3 mg kg^{-1}, I.V.), adequate anaesthesia was assessed by the absence (<5 mmHg) of blood pressure changes to a firm paw pinch. Rectal temperature was maintained at 37.5 ± 0.5°C.

Rats were tracheostomized and artificially ventilated. The vagus nerves were carefully dissected before sectioning but the aortic nerves were not identified. Inadvertent damage to one of these nerves could have occurred occasionally but this is unlikely given that the discharge of the renal nerve was robustly pulse-synchronous in all cases

examined. Femoral artery and vein were cannulated for BP recording and intravenous access, respectively. End-tidal CO_2 was monitored using a fast response time capnograph (Columbus Instruments, Columbus, OH, USA). The renal sympathetic nerve was freed from connective tissue, placed on a bipolar electrode and insulated for recording. The animals were placed prone in a Kopf stereotaxic frame with the bite bar set 3.5 mm below the interaural line.

Biotinamide-filled pipettes (0.5 M sodium acetate, 18–25 mΩ) were used to record and then label the recorded neurons with the juxtacellular method (Pinault, 1996; Schreihofer & Guyenet, 1997). To avoid damaging the transverse sinus, the A5 region was accessed through the parietal bone approximately 2.0 mm lateral to the midline and 1.5 mm rostral to the parieto-occipital suture using a 24 deg angle manipulator pointing to the rear of the animal. The A5 area is located rostral to the facial nucleus. In order to reach this area with accuracy, the rostral contour of the facial motor nucleus was mapped with field potentials elicited by stimulation of the mandibular branch of the facial nerve. The sampled region was from 1.8 to 2.3 mm lateral to the midline, and extended approximately 800 μm in the rostrocaudal direction including a roughly 200 μm stretch of A5 neuron-rich reticular formation located under the rostral end of the facial motor nucleus (Fig. 1*A*). Putative A5 neurons were tested for the presence of spinal axons since neuroanatomical evidence suggests that at least 93% of these cells send projections to the thoracic spinal cord (Byrum *et al.* 1984). For this purpose, the spinal cord was secured using a vertebral clamp placed at T4–T5 and a bipolar stimulation electrode was inserted at the T2–T3 level, approximately 1 mm below the dorsolateral sulcus on the ipsilateral side where the descending axons of the A5 neurons congregate.

All recorded neurons were tested for their sensitivity to hyperoxic hypercapnia, a measure of their direct or indirect reactivity to CNS acidification. The response of A5 and other nearby ventrolateral pontine neurons was tested under both isoflurane and urethane anaesthesia to ascertain that their sensitivity to increases in CNS P_{CO_2} was not anaesthetic dependent. Boluses of sodium cyanide (NaCN, 100 μg kg^{-1}, I.V.) were injected to test the neuronal responses to carotid body stimulation. These tests were performed in urethane-anaesthetized rats because the carotid body chemoreflex is virtually absent under isoflurane anaesthesia.

Optogenetic experiments

For these experiments we used a previously described lentiviral vector (PRSx8-ChR2-mCherry lenti) (Abbott *et al.* 2009*a*,*b*). This vector expresses an enhanced version of the photosensitive cationic channel channelrhodopsin-2 (ChR2 H134R, gift from Karl Deisseroth, Stanford, CA, USA) under the control of the artificial promoter PRSx8. ChR2 is fused to the reporter mCherry which can be detected without further processing or by immunohistochemistry using a rabbit anti-dsRed antibody (Abbott *et al.* 2009*a*,*b*). PRSx8 is a binding site for Phox2a or b and directs transgene expression selectively to neurons that express high levels of one or both of these transcription factors. Ponto-medullary noradrenergic or adrenergic neurons are among the cells that express high levels of transgene when exposed to PRSx8-containing viral vectors (Card *et al.* 2006; Abbott *et al.* 2009*a*,*b*; Pickering *et al.* 2009).

The lentivirus was injected into the A5 noradrenergic region of the ventrolateral pons in six rats that were anaesthetized with a mixture of ketamine (75 mg kg^{-1}), xylazine (5 mg kg^{-1}) and acepromazine (1 mg kg^{-1}) administered I.M. After surgery, the rats received injections of the antibiotic ampicillin (100 mg kg^{-1}, I.M.) and the analgesic ketorolac (0.6 mg kg^{-1}, I.P.) that were repeated the next day. The lentivirus was delivered by pressure through 25 μm outside diameter glass pipettes positioned at a 24 deg angle pointing towards the back of the animals. The pipettes were placed in a holder through which field potentials could be recorded and pressure pulses applied to eject the viral solution. Two injections (200 nl per site over 5 min) were made on the left side within the A5 region. The caudal injection was made at the rostral edge of the facial motor nucleus, a landmark that was determined by antidromic field potential recording as described above (coordinates: 2.0 mm lateral to the midline, 10–11.3 mm below the brain surface). The second injection was placed 400 μm rostral to the first at the same lateral coordinate, but 300 μm more dorsal. Physiological experiments were performed 15–20 days later. For these experiments the rats were prepared exactly as described in the previous section of the Methods except that multiunit activity of the lumbar sympathetic chain (L3–L4 level) was recorded along with that of the renal nerve. The lumbar sympathetic nerve chain was accessed via an abdominal opening that was closed following electrode placement.

All recordings were done while the rats were anaesthetized with 1.8–2% isoflurane delivered in pure oxygen. Photostimulation was done by inserting a 200 μm optical fibre along the same path used to inject the virus so as to position the tip above the midpoint between the two sites where virus had been injected. The light source was a diode-pumped 473 nm blue laser (CrystaLaser Model BC-473-060-M; Reno, NV, USA) controlled by a function generator (Grass Instruments, Warwick, RI, USA) to generate 20 ms light pulses. The power output was measured at the end of the fibre optic with a light-meter (Thorlabs, Newton, NJ, USA) and set at 9–12 mW when the laser was activated in continuous mode. Stimulation trials consisted of 30 s trains of 20 ms light pulses delivered

at 20 Hz or single or twin 20 ms light pulses delivered every 5–10 s.

Data acquisition and analysis

All analog data were acquired on a computer via a micro1401 digitizer (Cambridge Electronics (CED), Cambridge, UK) and were processed off-line using Spike 5 software (CED) as described (Guyenet *et al.* 2005). Renal and lumbar sympathetic nerve discharge (SND) were band-pass filtered (100–3000 Hz), rectified and integrated (time constant 1.2 ms for averaging responses evoked by single light pulses; time constant 2 s to measure the average effects of photostimulation at 20 Hz). SNDs were normalized within animals by assigning a value of 100 to resting SND and a value of 0 to the minimum value recorded during the silent period between bursts of activity.

Electrophysiological recording of A5 and A6 noradrenergic neurons in mouse brain slices

Transverse brainstem slices were prepared from neonatal mice (postnatal days 6–10) as described previously (Lazarenko *et al.* 2009). We used TH-GFP transgenic mice (Matsushita *et al.* 2002) in these experiments to identify the catecholaminergic neurons. Briefly, mice were anaesthetized with ketamine (375 mg kg^{-1}) and xylazine (25 mg kg^{-1}) I.P. and rapidly decapitated; brainstems were removed and slices (300 μm) cut in the transverse plane with a microslicer (DTK1000; Dosaka EM, Redding, CA, USA) in ice-cold substituted Ringer solution containing (in mM): 260 sucrose, 3 KCl, 5 $MgCl_2$, 1 $CaCl_2$, 1.25 NaH_2PO_4, 26 $NaHCO_3$, 10 glucose, and 1 kynurenic acid. Slices were incubated for 30 min at 35°C and subsequently at room temperature in a normal Ringer solution containing (in mM): 130 NaCl, 3 KCl, 2 $MgCl_2$, 2 $CaCl_2$, 1.25 NaH_2PO_4, 26 $NaHCO_3$, and 10 glucose. Both substituted and normal Ringer solutions were bubbled with 95% O_2 and 5% CO_2.

We targeted the GFP-fluorescent subpopulation of TH-expressing A5 and /or A6 (locus coeruleus) neurons for loose patch recordings of firing activity (Mulkey *et al.* 2004; Perkins, 2006). The slices were placed in a chamber on a fixed-stage fluorescence microscope (Axioskop FS; Zeiss) at room temperature (~24°C). Slices were continuously perfused (~3 ml min^{-1}) with normal Ringer solution (pH 7.3 when bubbled with 95% O_2 and 5% CO_2 at room temperature). Acidification of the bath solution (pH 6.9) was achieved by switching to a Ringer solution in which $NaHCO_3$ was replaced by NaCl to maintain iso-osmoticity ($NaHCO_3$ to 9.7 mM, NaCl to 146 mM). Patch electrodes had a DC resistance of 1.5–2.5 MΩ when filled with internal solution containing (mM): 152 NaCl, 3 KCl, 2 $MgCl_2$, 2 $CaCl_2$, 10 Hepes (pH 7.4), and 10 glucose.

Recordings were made with a Multiclamp 700B amplifier and a Digidata 1440A analog-to-digital converter with pCLAMP 10.0 software (all from Molecular Devices, Foster City, CA, USA). Integrated rate histograms were generated by binning action potentials in consecutive 10 s episodes in Spike 5.0 software. We report in Results the mean steady-state firing rate (spikes s^{-1}) calculated from the last 30 s of each pH change. Statistical analysis was performed using repeated measures ANOVA, with statistical significance at $P < 0.05$.

Histology

After each experiment *in vivo*, rats were deeply anaesthetized and then transcardially perfused with 4% paraformaldehyde. The brain was extracted and kept in 4% paraformaldehyde for 24–48 h. Brains were cut at room temperature on a vibrating microtome (Leica VT 1000S, Nussloch, Germany) into 30 μm transverse sections and stored in cryoprotectant at −20°C before further processing. All histological procedures were performed on free floating sections. ChR2-mCherry was detected with rabbit anti-dsRed (1:500; Clontech, Mountain View, CA, USA) followed by donkey-anti-rabbit IgG-Cy3 (1:200; Jackson ImmunoResearch Laboratories, Inc., West Grove, PA, USA). Biotinamide was detected with streptavidin-Alexa 488 (1:200; Invitrogen Life Sciences, Carlsbad, CA, USA) and tyrosine hydroxylase (TH) by immunohistochemistry using mouse monoclonal anti-TH (1:1000; Chemicon, Temecula, CA, USA) followed by either donkey anti-mouse IgG-Cy3 (1:200; Jackson) or donkey anti-mouse Ig-Alexa 488 (1:200; Invitrogen).

In vitro brain slices were fixed for 24–48 h in 4% paraformaldehyde and processed free-floating for detection of biotinamide with streptavidin-Alexa 488 (1:200; Invitrogen) and TH with mouse monoclonal anti-TH (1:1000; Chemicon) followed by donkey anti-mouse IgG-Cy3 (1:200; Jackson). All sections were mounted onto glass slides, dehydrated through a series of graded alcohols and xylenes and covered with DPX mounting medium (Fluka/Sigma-Aldrich, St Louis, MO, USA). The histological material was examined and photographed using a Zeiss Axioimager.Z1 (Carl Zeiss Microimaging, Thornwood, NY, USA) with a Zeiss Axiocam MRc digital camera (basic resolution 1388 pixels × 1040 pixels). To estimate the number and phenotype of transfected neurons, a one in six series of 30 μm-thick transverse sections that encompassed the transfected brain area (from 7–10 sections per rat) was plotted using the Neurolucida computer-assisted graphing software as previously described (Stornetta *et al.* 2002*b*).

Statistics

All values are presented as mean ± S.E.M. Statistical significance was set at $P < 0.05$. Unpaired t test, repeated measures ANOVA and two-way ANOVA were used as required. The Holm–Sidak method was used for all pair-wise comparisons.

Results

The A5 region contains two main types of active CO_2-sensitive neurons

Single units were recorded within the A5 region in six rats anaesthetized with isoflurane and four rats anaesthetized with urethane using the approach depicted in Fig. 1*A*. The sampled region contained two main types of active neurons. One type (Fig. 1*Ca–c*) had a very low level of discharge at the resting level of end-expiratory CO_2 of 3.8 ± 0.2% (0.98 ± 0.32 Hz; $n = 14$; range 0–3.5 Hz under isoflurane; 0.76 ± 0.29 Hz; $n = 10$; range 0.03–3.06 Hz under urethane, n.s. by t test). These neurons had a spinally projecting axon identified by the collision test (antidromic latency from thoracic segment T3: 32 ± 4 ms; range 12.3–74 ms; $n = 24$; estimated axonal conduction velocity: 0.92 ± 0.11 m s^{-1}; Fig. 1*Cb–d*). The discharge rate of these bulbospinal neurons was usually increased by hypercapnia (11 out 14 neurons recorded under isoflurane, 9 out of 10 neurons recorded under urethane) or unaffected by this stimulus. Figure 1*Ca–c* illustrates a bulbospinal neuron that was notably activated by CO_2 and Fig. 1*Cd* and *e* depicts a different bulbospinal neuron that was minimally affected by hypercapnia. On average, the activity of the bulbospinal neurons was mildly but significantly increased by CO_2 (repeated measures ANOVA, $P < 0.001$; Fig. 1*D*). The effect of CO_2 was not anaesthetic dependent ($P = 0.602$ by 2-way ANOVA, or $P = 0.143$ by t test when comparing the slope of the response to CO_2), therefore the data from Fig. 1*D* represent the pooled results of recordings obtained under both anaesthetics.

Only four bulbospinal A5 area neurons (out of 10 recorded under urethane) showed an arterial pulse modulation of their firing (Fig. 2*A*). The simultaneously recorded sympathetic nerve activity was always robustly synchronized to the blood pressure pulse (Fig. 2) indicating that arterial baroreceptors were active in all cases.

The other most common type of active neuron ($n = 10$ cells; 7 under isoflurane and 3 under urethane anaesthetic) encountered in the A5 region differed from the first in three respects. The discharge rate had a much larger dynamic range as a function of end-expiratory CO_2 than the bulbospinal neurons (representative example in Fig. 1*Ea* and *b*). Secondly, they could not be antidromically activated from the thoracic spinal cord. Finally, judging from their stereotaxic coordinates relative to the facial motor nucleus these CO_2-responsive neurons were located on average ventral to and more caudal than the bulbospinal neurons (Fig. 1*B*). The effect of CO_2 on these neurons is summarized in Fig. 1*D*. On average ($n = 10$ cells recorded in 7 rats), these neurons discharged at 2.0 ± 0.6 Hz at 3.7 ± 0.3% end-expiratory CO_2 and their activity increased by 2.8 ± 0.5 Hz for every additional 1% of end-expiratory CO_2. Their discharge rate was significantly higher than that of the bulbospinal neurons overall (2-way ANOVA, $P < 0.001$) but the difference was statistically significant only at high levels of CO_2 (5% and above; *post hoc* test by the Holm–Sidak method). The region in which these high-dynamic range CO_2-activated neurons were located corresponded to the rostral end of the retrotrapezoid nucleus, suggesting that these cells were retrotrapezoid chemoreceptors (Takakura *et al.* 2008).

A small number of active neurons with properties different from the two main categories of neurons noted above were also occasionally encountered in the region of interest including active and non-bulbospinal neurons that were insensitive to CO_2 ($n = 8$), 'pump' cells (neurons with respiratory phasic activity dependent on lung ventilation; $n = 3$) and active neurons that were inhibited by hypercapnia ($n = 2$).

The bulbospinal neurons of the A5 region express tyrosine hydroxylase (TH)

A subset of slowly discharging bulbospinal neurons was labelled juxtacellularly with biotinamide. Most of these cells (11/14) contained TH immunoreactivity (example of one neuron in Fig. 3*A*) indicating that they were noradrenergic since this region of the brain does not contain adrenergic or dopaminergic neurons. The labelled neurons were located under the rostrolateral edge of the facial motor nucleus or rostral and slightly dorsal to this landmark between the exit of the facial nerve and the superior olive (Fig. 3*B*). This region corresponds to the classically described A5 group of noradrenergic neurons (Andrade & Aghajanian, 1982; Byrum *et al.* 1984; Byrum & Guyenet, 1987).

A5 neurons are strongly activated by carotid body stimulation

Carotid body stimulation with cyanide produced a brief increase in splanchnic nerve activity peaking at 168 ± 14% of resting level and a vigorous stimulation of every A5 neuron sampled ($n = 7$ in 3 rats) (Fig. 4*A* and *B*).

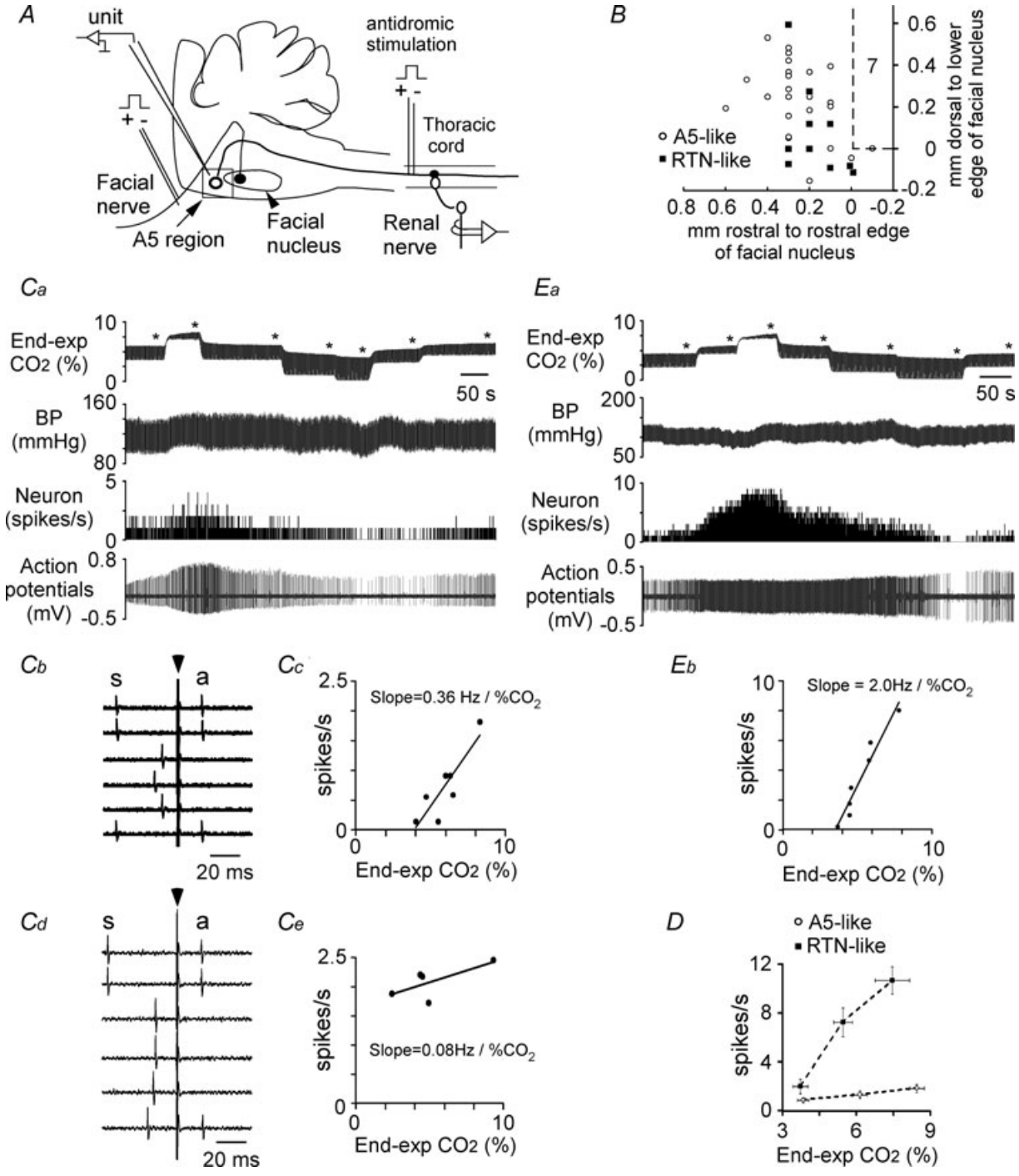

Figure 1. The A5 region contains two main types of CO_2-activated neurons
A, experimental design. Units were recorded in the ventrolateral pontine reticular formation. The region of interest was identified by its location relative to the facial motor nucleus. The presence of an axonal projection to the spinal cord was used as one of the criteria to identify putative A5 noradrenergic neurons. *B,* location of bulbospinal (putative noradrenergic) neurons and retrotrapezoid (RTN)-like neurons plotted as a function of their stereotaxic coordinates relative to the rostral and ventral edge of the facial motor nucleus (7) as monitored by antidromic field potentials. *C,* properties of bulbospinal A5 area neurons. *Ca,* response to step changes in end-expiratory CO_2; *Cb,* collision test showing that this neuron had an axon projecting to or through the thoracic spinal cord; *Cc,* relationship between unit discharge rate and end-expiratory CO_2 at steady state (from measurements taken where indicated by asterisks in panel *Ca*); *Cd*, collision test for a CO_2-insensitive A5 region neuron; *Ce,* relationship between unit discharge rate and end-expiratory CO_2 at steady state for the bulbospinal neuron shown in *Cd*.

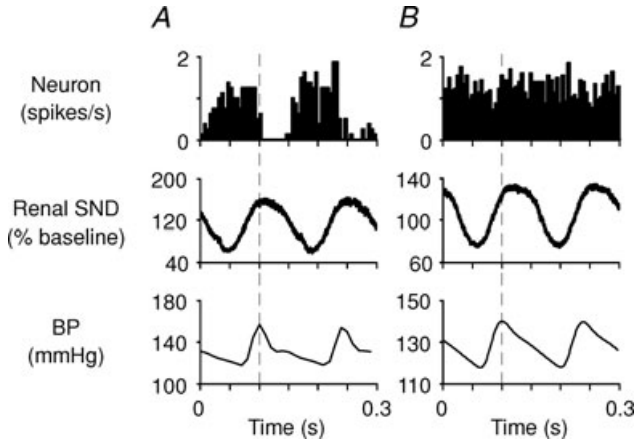

Figure 2. Cardiac rhythmicity of A5 neurons
Top graphs: peri-event activity histograms of two bulbospinal putative A5 neurons recorded under urethane anaesthesia (dashed line: trigger point on systolic BP signal; action potentials grouped into 5 ms bins). *A,* A5 cell with cardiac rhythmicity. *B,* A5 cell without cardiac-related modulation. Peri-event waveform averages of renal SND (rectified; middle panels) revealed a similar degree of pulse modulation of the sympathetic outflow in each case.

Photostimulation of A5 area ChR2-transfected neurons increases sympathetic tone

The cardiovascular effects elicited by photostimulation of ChR2-transfected A5 neurons (30 s trains, 20 Hz, 20 ms pulses, 9–12 mW) were examined in six rats. Renal SND was very slightly but significantly elevated ($3.5 \pm 0.6\%$; $P < 0.05$ by paired t test) but photostimulation had no effect on the mean lumbar SND nor on BP. Photostimulation at 10, 5 or 2 Hz had no effect on the mean integrated value of SND or on BP.

Low frequency photostimulation of the A5 region (20 ms pulses at 0.1 Hz) evoked a short-lasting increase in renal nerve activity followed by a period of inhibition (Fig. 5). A qualitatively similar but much smaller evoked response was observed in the lumbar sympathetic chain (Fig. 5). These effects were observed in every rat. On average ($n = 6$) the peak of activity evoked by photostimulation reached $197 \pm 10\%$ of the mean baseline discharge in the renal nerve *vs.* $127 \pm 4\%$ in the lumbar nerve ($P < 0.05$ by t test). The peak onset was shorter for renal (66 ± 4 ms) than lumbar SND (104 ± 2 ms; $P < 0.05$ by t test) as expected from the fact that the sympathetic

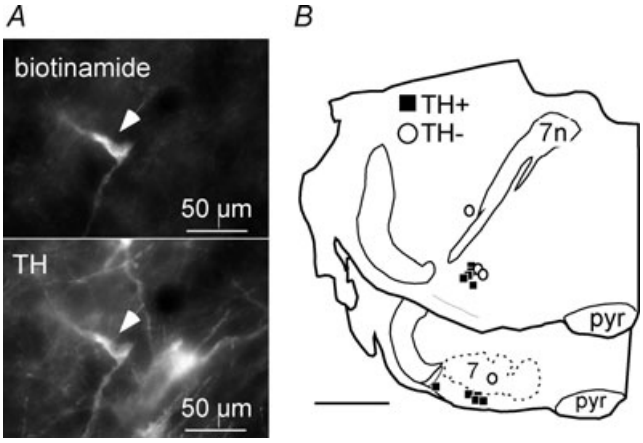

Figure 3. Identification of A5 neurons by juxtacellular labelling *in vivo*
A, top: single bulbospinal neuron labelled with biotinamide after electrophysiological characterization (Alexa 488 fluorescence). Bottom: same field showing that the recorded neurons contained tyrosine hydroxylase (TH) immunofluorescence (Cy3). *B*, computer-assisted plots of the location of 14 biotinamide-labelled neurons. Most (11/14) were TH-ir (filled squares). 7, facial motor nucleus; 7n, facial nerve.

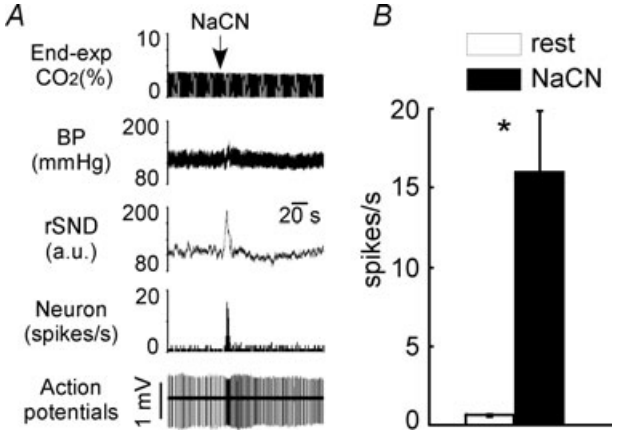

Figure 4. Activation of A5 noradrenergic neurons by intravenous cyanide
Boluses of sodium cyanide (NaCN) were administered to stimulate the carotid bodies (urethane-anaesthetized rats). *A*, effect of NaCN on one A5 neuron. From top to bottom: end-expiratory CO_2, arterial pressure, renal sympathetic nerve discharge rectified and integrated, integrated rate histogram of the discharge of a single A5 neuron, raw trace of extracellular action potentials. *B*, group data. Open bar: neuronal discharge rate at rest (averaged over 1 min; end-expiratory CO_2 close to 5.5%). Filled bar: maximal discharge rate observed during bolus administration of cyanide (1 s interval). $^*P < 0.05$ by t test relative to resting condition.

D, relationship between discharge rate and end-expiratory CO_2 at steady state for bulbospinal, putative A5 neurons ($n = 24$) and putative RTN neurons ($n = 10$). *E,* RTN-like neuron with high dynamic range of response to CO_2. *Ea,* response to step changes in end-expiratory CO_2; *Eb,* relationship between unit discharge rate and end-expiratory CO_2 at steady state (from measurements taken at asterisks in *Ea*).

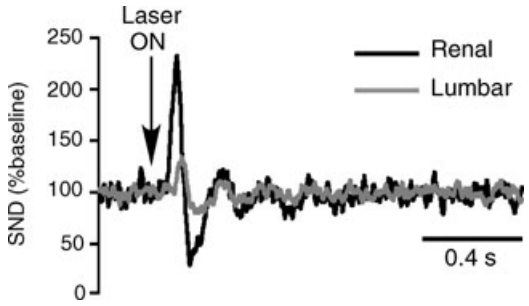

Figure 5. Sympathetic responses evoked by photostimulation of ChR2-transfected A5 area neurons
A, response evoked by 20 ms light pulses (at arrow) delivered every 5 s. SND was rectified, smoothed (1 ms time constant) and event-averaged using the onset of the light pulse as trigger (100 sweeps). The baseline was set at 100 arbitrary units for both nerves.

outflow to the lumbar chain originates from sympathetic preganglionic neurons that are located further down the spinal cord. Presumably for the same reason, the latency to peak was also shorter in the renal nerve (96 ± 4 ms) than in the lumbar nerve (125 ± 2 ms; $P < 0.05$ by t test). Post-peak inhibition was observed in both nerves. The magnitude of the inhibition was also larger for renal SND ($-43 \pm 6\%$ reduction from baseline) than lumbar SND ($-19 \pm 5\%$ from baseline; $P < 0.05$ by t test). The time to the post-peak inhibition was the same in both nerves (renal: 174 ± 6 ms; lumbar: 175 ± 7 ms).

Most ChR2-transfected neurons were located in the ventrolateral pons medial to the exit point of the facial nerve (Bregma –9.8 mm) and the majority of these neurons were immunoreactive (ir) for TH (Fig. 6*A* and *B*). Immediately adjacent superior olivary neurons and facial motor neurons were unlabelled. Figure 6 illustrates one case in which neuronal labelling was especially narrowly confined to the A5 region and over 89% of the cells (150 of 168) were TH-ir. In this particular case, single-pulse photostimulation produced a representative increase in renal SND (peak reaching 205% of baseline) and lumbar SND (121% of baseline). On average almost all ChR2-expressing neurons were TH-positive at the rostral end of the transfected region whereas TH-negative neurons were confined to the caudal end of the distribution (Fig. 6). The TH-negative neurons were located predominantly under the facial motor nucleus and had extensive superficial dendrites, a feature reminiscent of the previously described retrotrapezoid nucleus chemoreceptors (Mulkey *et al.* 2004).

The total number of ChR2-expressing neurons per rat was 264 ± 30 (range: 168–390; estimate based on cell counts made in every sixth section; 6 rats counted). The total number of TH-ir neurons positive for ChR2-mCherry was 174 ± 12 (average: 66% of total). The total population of A5 neurons per side in rats has been previously estimated at approximately 320 neurons (Byrum *et al.* 1984), therefore around half of the A5 neurons expressed ChR2. The tip of the optrode was found dorsal to the region that contained the largest number of ChR2-transfected neurons close to the exit point of the facial nerve (representative example in Fig. 6). Given that the TH-ir neurons (the A5 neurons) were on average located more dorsally than the TH-negative cells, the placement of the optrode should have favoured

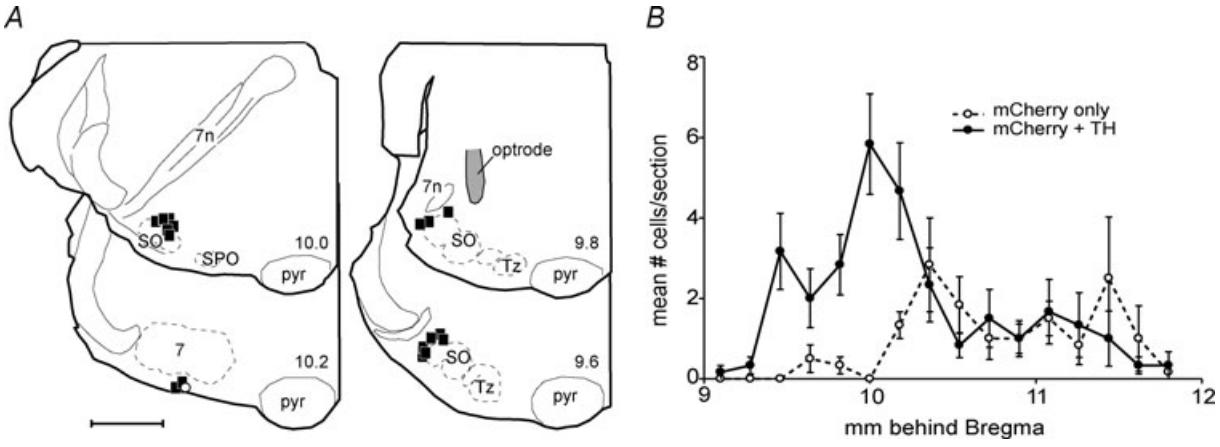

Figure 6. Anatomical distribution of channelrhodopsin-2-expressing neurons
A, computer-assisted plots of the distribution of ChR2-expressing neurons at four transverse planes of section in one rat in which over 90% of the neurons that expressed the transgene (mCherry positive) were TH-ir (filled squares). The numbers at the lower right of the hemisections refer to the approximate stereotaxic planes according to the atlas of Paxinos & Watson (2005). Abbreviations: pyr, pyramidal tract; SO, superior olive; SPO, superior paraolivary nucleus; Tz, nucleus of trapezoid body; 7, facial motor nucleus; 7n, facial nerve. The location of the tip of the fiberoptic is indicated in the upper right hemisection. *B*, rostrocaudal distribution of ChR2-expressing neurons in 6 rats (mean ± S.E.M.). ChR2-expressing non-catecholaminergic neurons (open circles) were located primarily within the retrotrapezoid nucleus, caudal to the bulk of the transfected A5 neurons (filled circles).

the illumination of the A5 neurons over that of the non-catecholaminergic cells.

Acid sensitivity of mouse A5 neurons in slices; comparison with locus coeruleus

There was considerable ectopic expression of GFP elsewhere in the lower brainstem of the TH-GFP transgenic mice (results not illustrated) but, within the A5 region of the pons, virtually every GFP-positive neuron was immunoreactive for TH (example in Fig. 7*A*). In three mice (3 transverse sections per mouse located close to the exit point of the facial nerve and separated by 180 μm), we identified 140 ± 30 GFP-positive A5 neurons (range 102–198) and only 12 ± 6 of those lacked detectable TH immunoreactivity (range 0–18). Therefore, at least 92% of the GFP-positive neurons located in this region of the pons were A5 noradrenergic neurons.

A5 neurons were recorded at room temperature in transverse slices cut from the pons of the TH-GFP transgenic mice. Replacing sodium bicarbonate with an equal amount of sodium chloride produced a 0.4 unit drop in perfusion medium pH from a resting pH of 7.3. This acidification increased reversibly but very modestly the discharge of the A5 neurons ($n = 8$ from 5 pups; Fig. 7*Ca*; $P < 0.001$, by repeated measures ANOVA). For comparison we also examined the acid sensitivity of locus coeruleus in slices from the same mice. These neurons were also significantly, albeit very weakly, activated in the presence of acid solution ($n = 11$ from 3 pups; Fig. 7*Cb*).

Juxtacellular labelling of a subset of recorded GFP-positive neurons located in the A5 region confirmed that the recorded cells did express TH ($n = 3$; Fig. 7*Ba* and *b*). Locus coeruleus identification in slices is obvious and therefore did not require *post hoc* histology.

Discussion

We show that the pontine reticular formation surrounding the rostral tip of the facial motor nucleus contains two main types of active neurons *in vivo*, A5 noradrenergic neurons and neurons with properties similar to the respiratory chemoreceptors identified previously in the rostral medulla oblongata (Mulkey *et al.* 2004). Among other distinguishing features, A5 neurons respond weakly to hyperoxic hypercapnia *in vivo* and negligibly to acidification in slices. Using an optogenetic approach, we confirmed that this region of the pontine reticular formation preferentially controls the visceral sympathetic outflow and we provided evidence that the A5 noradrenergic neurons contribute to this function. Given that the A5 neurons are vigorously excited by carotid body stimulation, we suggest that acute hypoxia may enhance visceral sympathetic nerve activity in part by

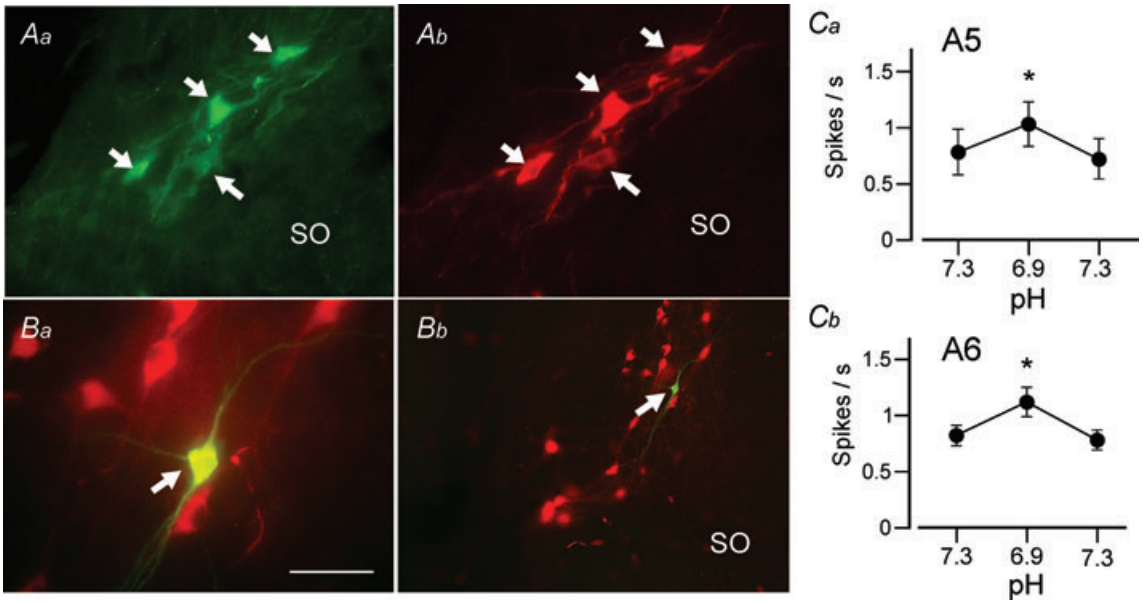

Figure 7. Activation of locus coeruleus and A5 neurons by metabolic acidosis in slices
A, selective expression of GFP by TH-ir neurons in the A5 region of the TH-GFP transgenic mouse used in all experiments (*Aa*, GFP immunoreactivity; *Ab*, TH immunoreactivity). *B*, example of one A5 neuron recorded in a slice and labelled with biotinamide (*Ba*, recorded, biotinamide-labelled neuron immunoreactive for TH surrounded by other A5 neurons; *Bb*, low magnification photograph showing the recorded neuron within the cluster of A5 neurons). Scale bar represents 50 μm in *Aa*, *Ab* and *Ba*, and 200 μm in *Bb*. *Ca*, small, reversible and statistically significant increase in the firing rate of A5 neurons exposed to metabolic acidosis in slices (isotonic reduction of bicarbonate at constant CO_2). *Cb*, identical experiment on locus coeruleus noradrenergic neurons.

activating the A5 neurons. Finally, although a contribution of A5 neurons to central respiratory chemoreflexes is not excluded, the ability of these neurons to directly detect changes in brain P_{CO_2} appears very limited.

Single-unit properties of the A5 neurons *in vivo*

The first single-unit recordings of putative A5 neurons were made by Andrade & Aghajanian (1982). These authors described slowly discharging neurons with triphasic action potentials reminiscent of locus coeruleus neurons which, like the latter cells, were strongly inhibited by local or systemic administration of α_2 adrenergic receptor agonists. Many of these neurons could be antidromically activated from the spinal cord and around 60% were inhibited by raising blood pressure (Andrade & Aghajanian, 1982). Later studies (Byrum *et al.* 1984; Huangfu *et al.* 1991) added that the spinal axons of these ventrolateral pontine neurons arborize preferentially in the region of the intermediolateral cell column and that their axons are damaged by the catecholamine neuron-selective toxin 6-hydroxydopamine (6-OHDA) (Loewy *et al.* 1979*b*; Byrum & Guyenet, 1987). This evidence supported the original interpretation that these bulbospinal neurons were noradrenergic (Andrade & Aghajanian, 1982) and the juxtacellular labelling experiments performed in the present study provide final proof that a clear majority of these slowly discharging bulbospinal neurons are indeed A5 noradrenergic neurons. However, around 20% of the bulbospinal neurons that we labelled did not express detectable levels of tyrosine hydroxylase. This observation could conceivably be a false negative result caused by the vagaries of the juxtacellular labelling method or by variations in the intensity of the tyrosine hydroxylase immunoreactivity amongst A5 neurons.

The original finding that only a portion of the A5 cells are inhibited by rises in blood pressure (Andrade & Aghajanian, 1982) has been replicated under other anaesthetic conditions (Huangfu *et al.* 1991). No more than half of these cells have a pulse-modulated discharge under conditions when arterial baroreceptors are clearly active as evidenced by the strong pulse modulation of the multiunit activity of the renal or splanchnic nerve (Huangfu *et al.* 1991 and present study). These congruent experimental results suggest that only a subset of the A5 neurons are under arterial baroreceptor control. The A5 region receives a moderately dense input from the C1 neurons (Card *et al.* 2006), which are in general strongly inhibited by arterial baroreceptor stimulation and highly pulse modulated (Schreihofer & Guyenet, 1997). The C1 cells are therefore a potential source of baroreceptor-regulated excitatory drive to some of the A5 neurons. The C1 neurons are also vigorously activated by peripheral chemoreceptor stimulation and weakly activated by hypercapnia (Sun, 1996; Moreira *et al.* 2006). These neurons could therefore account for or contribute to the response of A5 neurons to hypoxia and hypercapnia.

Sympathetic activation elicited by stimulation of channelrhodopsin-2-transfected A5 neurons

Electrical stimulation or microinjection of glutamate receptor agonists have been used to delineate the role of the A5 noradrenergic neurons in anaesthetized and conscious mammals (Loewy *et al.* 1979*a*; Neil & Loewy, 1982; Stanek *et al.* 1984; Maiorov *et al.* 1999) and in one study in awake rabbits, muscimol was injected to inhibit these neurons (Maiorov *et al.* 2000). The strong hypertensive effect produced by electrical stimulation of the A5 region of the pons was probably due to the activation of fibres of passage because they were not reproduced by administration of glutamate receptor agonists (Loewy *et al.* 1979*a*; Neil & Loewy, 1982; Stanek *et al.* 1984). The cardiovascular effects elicited by stimulation of the A5 region with glutamate or *N*-methyl D-aspartate were eventually attributed to a mix of sympathetically driven visceral vasoconstriction, hindlimb vasodilatation and cardiac output reduction that causes hypotension in awake rats and relatively little change in conscious rabbits and anaesthetized rats (Stanek *et al.* 1984; Huangfu *et al.* 1992; Maiorov *et al.* 1999). While the effects of NMDA were attenuated by somewhat selective lesions of the A5 neurons with 6-OHDA, it has been difficult to prove that they were entirely due to the activation of the A5 noradrenergic neurons as these cells are scattered at a low density within a region that is not clearly demarcated from the nearby pontine reticular formation and in addition, reside near the neuron-dense superior olivary complex and salivary nuclei.

The channelrhodopsin-2-based approach has the advantage of allowing histological identification of the population of neurons that is being potentially photo-activated (Arenkiel *et al.* 2007; Duale *et al.* 2007; Gradinaru *et al.* 2010). In the present case, due to the selectivity of the promoter PRSx8 for neurons that express the transcription factors Phox2a and or Phox2b, the transgene (ChR2-mCherry) was predominantly expressed by the A5 noradrenergic neurons (66% on average). However, non-catecholaminergic neurons were also transfected, most notably at the caudal end of the A5 region. This particular region harbours TH-negative Phox2b-expressing neurons that appear to be the rostral continuation of the retrotrapezoid nucleus (RTN) (Smith *et al.* 1989; Takakura *et al.* 2008; Guyenet & Mulkey, 2010). Accordingly, we found that this region contains highly CO_2-sensitive neurons with discharge characteristics that were reminiscent of the cells located at the better-characterized caudal end of the RTN

(Mulkey *et al.* 2004; Stornetta *et al.* 2006). RTN neurons express a high level of the transgene when exposed to PRSx8-ChR2-mCherry lentivirus (Abbott *et al.* 2009*a*) and they have no spinal projections (Kang *et al.* 2007). Accordingly, we assume that most of the non-catecholaminergic neurons that expressed ChR2 in the present experiments were RTN chemoreceptors.

Photostimulation of the ChR2-expressing neurons of the A5 region increased visceral sympathetic nerve activity, consistent with every previous study in which this pontine region has been activated with a glutamate receptor agonist (Stanek *et al.* 1984; Huangfu *et al.* 1992; Maiorov *et al.* 1999). Photostimulation at the maximal practical frequency of 20 Hz produced a much smaller mean increase in SND than NMDA or glutamate, however (Huangfu *et al.* 1992). This quantitative difference has two possible interpretations. Photostimulation may have activated only a very small fraction of the neurons that expressed detectable levels of ChR2-mCherry or the large visceral vasoconstriction and sympathoactivation elicited by activating ventrolateral pontine neurons with glutamate or NMDA results from the activation of cells other than the A5 neurons (olivary complex, other reticular formation neurons).

A second difference between present and past attempts at stimulating A5 neurons is that photostimulation did not inhibit lumbar sympathetic nerve activity but produced a small activation in our case. These results do not support the idea that activation of the A5 noradrenergic neurons inhibits sympathetic activity to hindlimb muscles as suggested by previous experiments using NMDA or glutamate (Stanek *et al.* 1984; Huangfu *et al.* 1992). The hindlimb muscle vasodilatation caused by NMDA injection into the ventrolateral pons may therefore be due to some kind of defence reaction (Hilton & Redfern, 1986) elicited by the activation of neurons other than the A5 noradrenergic cells. Alternatively, hindlimb vasodilatation may be triggered by a subset of A5 neurons that were not transfected with ChR2 in our experiments.

Low frequency photostimulation of ChR2-transfected A5 neurons evoked a short-lasting peak of sympathetic nerve activity not unlike the response evoked by photostimulating ChR2-transfected C1 neurons (Abbott *et al.* 2009*b*; Kanbar *et al.* 2010). Although, the amplitude of the response evoked by A5 stimulation was small, the evoked peak had a similar duration, a comparable latency and it was followed by a period of inhibition during which paired pulse inhibition was also observed (results not shown). The similarity in latencies can be explained by the fact that the axonal conduction velocity of A5 neurons and of the fastest contingent of C1 neurons is comparable (Morrison *et al.* 1988; Schreihofer & Guyenet, 1997; Kanbar *et al.* 2010). However, the fact that a short-lasting excitatory peak was produced suggests that the A5 neurons could be releasing some as yet uncharacterized fast-acting excitatory transmitter since noradrenaline does not produce a detectable EPSP in sympathetic preganglionic neurons, but merely changes the intrinsic properties of these neurons (Sah & McLachlan, 1995). Glutamate is unlikely to be the fast transmitter released by the A5 noradrenergic neurons because these cells contain neither vesicular glutamate transporter 1 (VGLUT1) nor VGLUT2 and VGLUT3 mRNA is undetectable in the pons (Stornetta *et al.* 2002*a*,*b*; Herzog *et al.* 2004). ATP is a candidate since this substance is released by other catecholaminergic cells such as postganglionic sympathetic neurons, adrenal medullary cells and the principal cells of the carotid bodies (Burnstock, 2009; Nurse, 2010). This hypothesis is compatible with the persistence of a fast EPSP evoked by lateral funiculus stimulation in sympathetic preganglionic neurons after blockade of glutamatergic receptors with CNQX (Sah & McLachlan, 1995), although these authors did not exclude NMDA receptors as a potential explanation for the CNQX-resistant EPSP.

The finding that A5 neurons control visceral sympathetic tone is consistent with anatomical data (Strack *et al.* 1989; Schramm *et al.* 1993). However, these pseudorabies virus studies suggest that A5 neurons also target many other types of sympathetic preganglionic neurons including those that control skeletal muscle blood flow (e.g. Rotto-Percelay *et al.* 1992). The simplest way to reconcile these anatomical observations with the present physiological findings would be to assume that A5 neurons target sympathetic preganglionic neurons indiscriminately but that they activate these cells to varying degrees according to which organ they regulate, e.g. kidney more than skeletal muscle efferents. Another possibility is that the A5 neurons are organized into functional subgroups, like the C1 neurons (McAllen *et al.* 1997), and that we photostimulated a cluster of A5 neurons that happens to control visceral sympathetic tone preferentially. Experimental support for distinct functional subgroups of A5 neurons is limited. The fact that only half of the A5 neurons receive detectable baroreceptor inputs may be a hint. The final possibility is that the changes in sympathetic nerve activity that we elicited by photostimulating the ChR2-transfected neurons were caused by the activation of the RTN-like neurons rather than the A5 cells. Although RTN neurons are best known for their role in breathing regulation (Guyenet, 2008; Guyenet & Mulkey, 2010), these cells are glutamatergic, innervate the region of the ventrolateral medulla and could change sympathetic efferent activity by activating the C1 and other presympathetic neurons that reside in this region (Abbott *et al.* 2009*a*). This interpretation cannot be discounted at present. It is the least likely, however, because the majority of the ChR2-expressing neurons were A5 neurons, the optrode placement was located above the region that contained predominantly A5-labelled neurons and, in one

rat in which 89% of the transfected neurons were A5 cells, photostimulation still evoked an above-average response in the renal nerve.

Pontine noradrenergic neurons and the chemoreflexes

The locus coeruleus (A6) is considered to have a central respiratory chemoreceptor function because these cells are mildly activated by hypercapnia and by acidification *in vitro* and because chronic lesions of this nucleus attenuate the breathing stimulation elicited by hypercapnia (Pineda & Aghajanian, 1997; Ritucci *et al.* 2005; Biancardi *et al.* 2008; Nichols *et al.* 2008; Nattie & Li, 2009). The locus coeruleus is also activated by carotid body stimulation (hypoxia or cyanide) (Elam *et al.* 1981; Teppema *et al.* 1997) but, oddly, lesions of this structure have no effect on the peripheral respiratory chemoreflex (Biancardi *et al.* 2010).

The present study indicates that the A5 and locus coeruleus neurons have similarly low acid sensitivity in slices and similarly modest sensitivity to hypercapnia *in vivo* (Elam *et al.* 1981; Nichols *et al.* 2008). The acid sensitivity of pontine noradrenergic neurons is best compared with that of the central respiratory chemoreceptors located in the retrotrapezoid nucleus recorded under exactly the same conditions using mice of the same age. The latter neurons display a more than 10-fold larger dynamic range of response to acid than A5 or A6 neurons, expressed as spikes per second per pH unit (Lazarenko *et al.* 2009). Neuronal acid sensitivity increases during the postnatal period in rodents and also increases with temperature, perhaps because of the contribution of glial cells to this process (Gourine *et al.* 2010). For these reasons, our *in vitro* results certainly underestimate the sensitivity of mature pontine noradrenergic neurons to local changes in pH. However, as shown in this and previous studies, the dynamic range of the response of A5 and locus coeruleus neurons to hypercapnia *in vivo* is also at least 10-fold smaller to that of the RTN (Guyenet *et al.* 2005).

The fact that ventrolateral pontine bulbospinal neurons are excited by carotid body stimulation is already documented (Huangfu *et al.* 1991). We show here that this property is a general characteristic of the A5 noradrenergic neurons, regardless of whether these cells respond to hyperoxic hypercapnia or receive baroreceptor inputs. The result is consistent with the fact that the majority of A5 neurons express c-Fos in animals exposed to hypoxia (Hirooka *et al.* 1997; Teppema *et al.* 1997).

In anaesthetized rats, the activation of visceral SND by carotid body stimulation (carotid chemoreflex) is attenuated by inhibiting the A5 region with muscimol and this effect is no longer observed after destruction of the A5 neurons and other pontomedullary noradrenergic neurons with 6-OHDA (Koshiya & Guyenet, 1994). Accordingly, A5 neurons seem to mediate or at least facilitate a portion of the carotid chemoreflex. This interpretation is compatible with the present finding that the A5 neurons are vigorously activated by carotid body stimulation. However, Koshiya & Guyenet (1994) found no evidence that the release of noradrenaline in the spinal cord contributed to the carotid body reflex since intrathecal administration of α- or β-adrenergic antagonists had no effect on its magnitude. The present experiments also raise doubt that the short-lasting excitatory response evoked by photostimulation of the A5 neurons could be due to the release of noradrenaline. These contradictions could again be explained by the possibility that A5 neurons, like the C1 neurons, release a non-catecholaminergic fast-acting transmitter and that this transmitter is primarily responsible for the short-term effects caused by the activation of these neurons. Another possibility is that the A5 neurons, which innervate numerous brain regions besides the lateral horn of the spinal cord (Byrum & Guyenet, 1987), activate sympathetic efferents primarily by recruiting non-catecholaminergic neurons.

Conclusion

In the conscious state, intense stimulation of the carotid bodies produces an alerting-defence response comparable to that elicited by nociceptive stimuli of somatic origin (Marshall, 1994). A5 neurons are activated by both types of stimuli (Andrade & Aghajanian, 1982). This activation could conceivably be a non-specific and stereotyped response to potentially aversive stimuli. Consistent with this interpretation, the alerting-defence response is characterized by intense visceral vasoconstriction and A5 neuron stimulation increases visceral sympathetic tone preferentially. However, there is also evidence that A5 neurons can be activated by relatively moderate hypoxia (12%) (Guyenet *et al.* 1993) suggesting that these neurons may also be responsive to smaller and more physiologically relevant changes in peripheral chemoreceptor stimulation in the conscious state.

References

Abbott SBG, Stornetta RL, Fortuna MG, Depuy SD, West GH, Harris TE & Guyenet PG (2009*a*). Photostimulation of retrotrapezoid nucleus Phox2b-expressing neurons *in vivo* produces long-lasting activation of breathing in rats. *J Neurosci* **29**, 5806–5819.

Abbott SBG, Stornetta RL, Socolovsky CS, West GH & Guyenet PG (2009*b*). Photostimulation of channelrhodopsin-2 expressing ventrolateral medullary neurons increases sympathetic nerve activity and blood pressure in rats. *J Physiol* **587**, 5613–5631.

Andrade R & Aghajanian GK (1982). Single cell activity in the noradrenergic A-5 region: Responses to drugs and peripheral manipulations of blood pressure. *Brain Res* **242**, 125–135.

Arenkiel BR, Peca J, Davison IG, Feliciano C, Deisseroth K, Augustine GJ, Ehlers MD & Feng G (2007). In vivo light-induced activation of neural circuitry in transgenic mice expressing channelrhodopsin-2. *Neuron* **54**, 205–218.

Aston-Jones G, Chen S, Zhu Y & Oshinsky ML (2001). A neural circuit for circadian regulation of arousal. *Nat Neurosci* **4**, 732–738.

Aston-Jones G, Rajkowski J & Cohen J (1999). Role of locus coeruleus in attention and behavioral flexibility. *Biol Psychiatry* **46**, 1309–1320.

Biancardi V, Bicego KC, Almeida MC & Gargaglioni LH (2008). Locus coeruleus noradrenergic neurons and CO_2 drive to breathing. *Pflugers Arch* **455**, 1119–1128.

Biancardi V, da Silva LT, Bicego KC & Gargaglioni LH (2010). Role of locus coeruleus noradrenergic neurons in cardiorespiratory and thermal control during hypoxia. *Respir Physiol Neurobiol* **170**, 150–156.

Burnstock G (2009). Purinergic cotransmission. *Exp Physiol* **94**, 20–24.

Byrum CE & Guyenet PG (1987). Afferent and efferent connections of the A5 noradrenergic cell group in the rat. *J Comp Neurol* **261**, 529–542.

Byrum CE, Stornetta R & Guyenet PG (1984). Electrophysiological properties of spinally-projecting A5 noradrenergic neurons. *Brain Res* **303**, 15–29.

Card JP, Sved JC, Craig B, Raizada M, Vazquez J & Sved AF (2006). Efferent projections of rat rostroventrolateral medulla C1 catecholamine neurons: Implications for the central control of cardiovascular regulation. *J Comp Neurol* **499**, 840–859.

Duale H, Waki H, Howorth P, Kasparov S, Teschemacher AG & Paton JF (2007). Restraining influence of A2 neurons in chronic control of arterial pressure in spontaneously hypertensive rats. *Cardiovasc Res* **76**, 184–193.

Elam M, Yao T, Thoren P & Svensson TH (1981). Hypercapnia and hypoxia: chemoreceptor-mediated control of locus coeruleus neurons and splanchnic sympathetic nerve. *Brain Res* **222**, 373–381.

Gourine AV, Kasymov V, Marina N, Tang F, Figueiredo MF, Lane S, Teschemacher AG, Spyer KM, Deisseroth K & Kasparov S (2010). Astrocytes control breathing through pH-dependent release of ATP. *Science* **329**, 571–575.

Gradinaru V, Zhang F, Ramakrishnan C, Mattis J, Prakash R, Diester I, Goshen I, Thompson KR & Deisseroth K (2010). Molecular and cellular approaches for diversifying and extending optogenetics. *Cell* **141**, 154–165.

Guyenet PG (2008). The 2008 Carl Ludwig Lecture: retrotrapezoid nucleus, CO_2 homeostasis, and breathing automaticity. *J Appl Physiol* **105**, 404–416.

Guyenet PG, Koshiya N, Huangfu D, Verberne AJM & Riley TA (1993). Central respiratory control of A5 and A6 pontine noradrenergic neurons. *Am J Physiol Regul Integr Comp Physiol* **264**, R1035–R1044.

Guyenet PG & Mulkey DK (2010). Retrotrapezoid nucleus and parafacial respiratory group. *Respir Physiol Neurobiol* **173**, 244–255.

Guyenet PG, Mulkey DK, Stornetta RL & Bayliss DA (2005). Regulation of ventral surface chemoreceptors by the central respiratory pattern generator. *J Neurosci* **25**, 8938–8947.

Hartzler LK, Dean JB & Putnam RW (2008). The chemosensitive response of neurons from the locus coeruleus (LC) to hypercapnic acidosis with clamped intracellular pH. *Adv Exp Med Biol* **605**, 333–337.

Herzog E, Gilchrist J, Gras C, Muzerelle A, Ravassard P, Giros B, Gaspar P & El Mestikawy S (2004). Localization of VGLUT3, the vesicular glutamate transporter type 3, in the rat brain. *Neuroscience* **123**, 983–1002.

Hilaire G, Viemari JC, Coulon P, Simonneau M & Bevengut M (2004). Modulation of the respiratory rhythm generator by the pontine noradrenergic A5 and A6 groups in rodents. *Respir Physiol Neurobiol* **143**, 187–197.

Hilton SM & Redfern WS (1986). A search for brain stem cell groups integrating the defence reaction in the rat. *J Physiol* **378**, 213–228.

Hirooka Y, Polson JW, Potts PD & Dampney RAL (1997). Hypoxia-induced Fos expression in neurons projecting to the pressor region in the rostral ventrolateral medulla. *Neuroscience* **80**, 1209–1224.

Huangfu D, Hwang LJ, Riley TA & Guyenet PG (1992). Splanchnic nerve response to A5-area stimulation in rats. *Am J Physiol Regul Integr Comp Physiol* **263**, R437–R446.

Huangfu D, Koshiya N & Guyenet PG (1991). A5 noradrenergic unit activity and sympathetic nerve discharge in rats. *Am J Physiol Regul Integr Comp Physiol* **261**, R393–R402.

Hwang DY, Carlezon WA Jr, Isacson O & Kim KS (2001). A high-efficiency synthetic promoter that drives transgene expression selectively in noradrenergic neurons. *Hum Gene Ther* **12**, 1731–1740.

Kanbar R, Stornetta RL, Cash DR, Lewis SJ & Guyenet PG (2010). Photostimulation of Phox2b medullary neurons activates cardiorespiratory function in conscious rats. *Am J Respir Crit Care Med* **182**, 1184–1194.

Kang BJ, Chang DA, Mackay DD, West GH, Moreira TS, Takakura AC, Gwilt JM, Guyenet PG & Stornetta RL (2007). Central nervous system distribution of the transcription factor Phox2b in the adult rat. *J Comp Neurol* **503**, 627–641.

Koshiya N & Guyenet PG (1994). A5 noradrenergic neurons and the carotid sympathetic chemoreflex. *Am J Physiol Regul Integr Comp Physiol* **267**, R519–R526.

Lazarenko RM, Milner TA, Depuy SD, Stornetta RL, West GH, Kievits JA, Bayliss DA & Guyenet PG (2009). Acid sensitivity and ultrastructure of the retrotrapezoid nucleus in Phox2b-EGFP transgenic mice. *J Comp Neurol* **517**, 69–86.

Li A, Emond L & Nattie E (2008). Brainstem catecholaminergic neurons modulate both respiratory and cardiovascular function. *Adv Exp Med Biol* **605**, 371–376.

Loewy AD, Gregorie EM, McKellar S & Baker RP (1979*a*). Electrophysiological evidence that the A5 catecholaminergic cell group is a vasomotor center. *Brain Res* **178**, 196–200.

Loewy AD, McKellar S & Saper CB (1979*b*). Direct projections from the A5 catecholamine cell group to the intermediolateral cell column. *Brain Res* **174**, 309–314.

McAllen RM, May CN & Campos RR (1997). The supply of vasomotor drive to individual classes of sympathetic neuron. *Clin Exp Hypertens* **19**, 607–618.

Maiorov DN, Malpas SC & Head GA (2000). Influence of pontine A5 region on renal sympathetic nerve activity in conscious rabbits. *Am J Physiol Reg Integr Comp Physiol* **278**, R311–R319.

Maiorov DN, Wilton ER, Badoer E, Petrie D, Head GA & Malpas SC (1999). Sympathetic response to stimulation of the pontine A5 region in conscious rabbits. *Brain Res* **815**, 227–236.

Marshall JM (1994). Peripheral chemoreceptors and cardiovascular regulation. *Physiol Rev* **74**, 543–594.

Matsushita N, Okada H, Yasoshima Y, Takahashi K, Kiuchi K & Kobayashi K (2002). Dynamics of tyrosine hydroxylase promoter activity during midbrain dopaminergic neuron development. *J Neurochem* **82**, 295–304.

Moreira TS, Takakura AC, Colombari E & Guyenet PG (2006). Central chemoreceptors and sympathetic vasomotor outflow. *J Physiol* **577**, 369–386.

Morrison SF, Milner TA & Reis DJ (1988). Reticulospinal vasomotor neurons of the rat rostral ventrolateral medulla: relationship to sympathetic nerve activity and the C1 adrenergic cell group. *J Neurosci* **8**, 1286–1301.

Mulkey DK, Stornetta RL, Weston MC, Simmons JR, Parker A, Bayliss DA & Guyenet PG (2004). Respiratory control by ventral surface chemoreceptor neurons in rats. *Nat Neurosci* **7**, 1360–1369.

Nattie E & Li A (2009). Central chemoreception is a complex system function that involves multiple brain stem sites. *J Appl Physiol* **106**, 1464–1466.

Neil JJ & Loewy AD (1982). Decreases in blood pressure in response to L-glutamate microinjections into the A5 catecholamine cell group. *Brain Res* **241**, 271–278.

Nichols NL, Hartzler LK, Conrad SC, Dean JB & Putnam RW (2008). Intrinsic chemosensitivity of individual nucleus tractus solitarius (NTS) and locus coeruleus (LC) neurons from neonatal rats. *Adv Exp Med Biol* **605**, 348–352.

Nurse CA (2010). Neurotransmitter and neuromodulatory mechanisms at peripheral arterial chemoreceptors. *Exp Physiol* **95**, 657–667.

Paxinos G & Watson C (2005). *The Rat Brain in Stereotaxic Coordinates*. Elsevier Academic Press, San Diego.

Perkins KL (2006). Cell-attached voltage-clamp and current-clamp recording and stimulation techniques in brain slices. *J Neurosci Methods* **154**, 1–18.

Pickering AE, Thornton SR, Love-Jones SJ, Steeds C & Patel NK (2009). Analgesia in conjunction with normalisation of thermal sensation following deep brain stimulation for central post-stroke pain. *Pain* **147**, 299–304.

Pinault D (1996). A novel single-cell staining procedure performed in vivo under electrophysiological control: morpho-functional features of juxtacellularly labeled thalamic cells and other central neurons with biocytin or Neurobiotin. *J Neurosci Methods* **65**, 113–136.

Pineda J & Aghajanian GK (1997). Carbon dioxide regulates the tonic activity of locus coeruleus neurons by modulating a proton- and polyamine-sensitive inward rectifier potassium current. *Neuroscience* **77**, 723–743.

Ritucci NA, Dean JB & Putnam RW (2005). Somatic *vs.* dendritic responses to hypercapnia in chemosensitive locus coeruleus neurons from neonatal rats. *Am J Physiol Cell Physiol* **289**, C1094–C1104.

Rotto-Percelay DM, Wheeler JG, Osorio FA, Platt KB & Loewy AD (1992). Transneuronal labeling of spinal interneurons and sympathetic preganglionic neurons after pseudorabies virus injections in the rat medial gastrocnemius muscle. *Brain Res* **574**, 291–306.

Sah P & McLachlan EM (1995). Membrane properties and synaptic potentials in rat sympathetic preganglionic neurons studied in horizontal spinal cord slices in vitro. *J Auton Nerv Syst* **53**, 1–15.

Schramm LP, Strack AM, Platt KB & Loewy AD (1993). Peripheral and central pathways regulating the kidney: a study using pseudorabies virus. *Brain Res* **616**, 251–262.

Schreihofer AM & Guyenet PG (1997). Identification of C1 presympathetic neurons in rat rostral ventrolateral medulla by juxtacellular labeling in vivo. *J Comp Neurol* **387**, 524–536.

Smith JC, Morrison DE, Ellenberger HH, Otto MR & Feldman JL (1989). Brainstem projections to the major respiratory neuron populations in the medulla of the cat. *J Comp Neurol* **281**, 69–96.

Stanek KA, Neil JJ, Sawyer WB & Loewy AD (1984). Changes in regional blood flow and cardiac output after L-glutamate stimulation of A5 cell group. *Am J Physiol Heart Circ Physiol* **246**, H44–H51.

Stornetta RL, Moreira TS, Takakura AC, Kang BJ, Chang DA, West GH, Brunet JF, Mulkey DK, Bayliss DA & Guyenet PG (2006). Expression of Phox2b by brainstem neurons involved in chemosensory integration in the adult rat. *J Neurosci* **26**, 10305–10314.

Stornetta RL, Sevigny CP & Guyenet PG (2002*a*). Vesicular glutamate transporter DNPI/VGLUT2 mRNA is present in C1 and several other groups of brainstem catecholaminergic neurons. *J Comp Neurol* **444**, 191–206.

Stornetta RL, Sevigny CP, Schreihofer AM, Rosin DL & Guyenet PG (2002*b*). Vesicular glutamate transporter DNPI/GLUT2 is expressed by both C1 adrenergic and nonaminergic presympathetic vasomotor neurons of the rat medulla. *J Comp Neurol* **444**, 207–220.

Strack AM, Sawyer WB, Hughes JH, Platt KB & Loewy AD (1989). A general pattern of CNS innervation of the sympathetic outflow demonstrated by transneuronal pseudorabies viral infections. *Brain Res* **491**, 156–162.

Sun MK (1996). Pharmacology of reticulospinal vasomotor neurons in cardiovascular regulation. *Pharmacol Rev* **48**, 465–494.

Takakura AC, Moreira TS, Stornetta RL, West GH, Gwilt JM & Guyenet PG (2008). Selective lesion of retrotrapezoid Phox2b-expressing neurons raises the apnoeic threshold in rats. *J Physiol* **586**, 2975–2991.

Teppema LJ, Veening JG, Kranenburg A, Dahan A, Berkenbosch A & Olievier C (1997). Expression of *c-fos* in the rat brainstem after exposure to hypoxia and to normoxic and hyperoxic hypercapnia. *J Comp Neurol* **388**, 169–190.

Zanella S, Roux JC, Viemari JC & Hilaire G (2006). Possible modulation of the mouse respiratory rhythm generator by A1/C1 neurones. *Respir Physiol Neurobiol* **153**, 126–138.

Author contributions

All experiments were performed at the Department of Pharmacology, University of Virginia. R.K., S.D.D., R.L.S. and P.G.G. conceived and designed the experiments. R.K., S.D.D., R.L.S., G.H.W. and P.G.G. collected, analysed and interpreted the data. R.L.S. and P.G.G. drafted the article and revised it critically for important intellectual content. All authors approved the final version of the manuscript.

Acknowledgements

This work was supported by grants from the National Institutes of Health (HL28785 and HL74011 to P.G.G.). Our thanks to Dr Kazuto Kobayashi, Department of Molecular Genetics, Institute of Biomedical Sciences, Fukushima Medical University School of Medicine, for the use of his TH-GFP mice and to Karl Deisseroth, Stanford University, for the channelrhodopsin construct.